nature energy

REVIEW ARTICLE

https://doi.org/10.1038/s41560-020-00761-x



# Designing anion exchange membranes for $CO_2$ electrolysers

Danielle A. Salvatore[1,12], Christine M. Gabardo[2,12], Angelica Reyes[1,12], Colin P. O'Brien[2,12], Steven Holdcroft[3], Peter Pintauro[4], Bamdad Bahar[5], Michael Hickner[6], Chulsung Bae[7], David Sinton[2], Edward H. Sargent[8] and Curtis P. Berlinguette[1,9,10,11] ✉

**New technologies are required to electrocatalytically convert carbon dioxide ($CO_2$) into fuels and chemicals at near-ambient temperatures and pressures more effectively. One particular challenge is mediating the electrochemical $CO_2$ reduction reaction ($CO_2$RR) at low cell voltages while maintaining high conversion efficiencies. Anion exchange membranes (AEMs) in zero-gap reactors offer promise in this direction; however, there remain substantial obstacles to be overcome in tailoring the membranes and other cell components to the requirements of $CO_2$RR systems. Here we review recent advances, and remaining challenges, in AEM materials and devices for $CO_2$RR. We discuss the principles underpinning AEM operation and the properties desired for $CO_2$RR, in addition to reviewing state-of-the-art AEMs in $CO_2$ electrolysers. We close with future design strategies to minimize product crossover, improve mechanical and chemical stability, and overcome the energy losses associated with the use of AEMs for $CO_2$RR systems.**

A global effort seeks to design electrochemical reactors that selectively reduce carbon dioxide ($CO_2$) at high reaction rates and energy efficiencies. The design of a $CO_2$ electrolyser that operates at current densities >200 mA cm$^{-2}$ and voltages <3 V will be required to provide the efficiency, selectivity, robustness and economic viability required for industrial applications[1,2]. The membrane, a core component of $CO_2$ electrolyser technology, must facilitate ion transport between the anode and cathode and chemically isolate the two half-cell reactions.

Electrochemical $CO_2$ reduction has been achieved in several reactor architectures, including the zero-gap reactor (or membrane electrode assembly) originally developed for low-temperature water electrolysis and fuel-cell systems[1,3,4]. The zero-gap reactor contains a cathode and anode pressed tightly onto opposite sides of a 10–150-μm-thick ion exchange membrane. Ohmic losses are minimized by decreasing the distance between these electrodes in the zero-gap reactor. These reactors also alleviate mass transport limitations that arise in aqueous $CO_2$ feedstocks, and continuously deliver gaseous $CO_2$ through a gas diffusion electrode (GDE) for reaction at the membrane/cathode interface[1]. The anode is typically fed with an aqueous electrolyte (for example, KOH, $KHCO_3$, $H_2O$) to perform the oxygen evolution reaction.

Three broad classes of membranes that have been tested in $CO_2$ flow reactors include anion exchange membranes (AEMs)[5], cation exchange membranes (CEMs)[6] and bipolar membranes (BPMs)[7]. The choice of membrane in zero-gap reactors will affect the pH on both sides of the membrane, thereby affecting reactant availability and reaction potentials for the cathodic and anodic reactions. CEMs generally transport cations from an acidic anode to the cathode and AEMs transport anions from a basic cathode to the anode. BPMs enable the dissociation of $H_2O$ and transport $H^+$ to the cathode and $OH^-$ to the anode under 'reverse bias' (that is, anion exchange layer facing the anode and cation exchange layer facing the cathode), or transport $H^+$ from the anode and $OH^-$ from the cathode and form water at the centre of the membrane under 'forward bias' (that is, anion exchange layer facing the cathode and cation exchange layer facing the anode)[8].

As discussed in more detail below, there is a reaction between the $CO_2$ and the locally generated $OH^-$ at the cathode, producing $HCO_3^-$ and $CO_3^{2-}$. These $HCO_3^-$ and $CO_3^{2-}$ anions are conducted through the AEM to the locally acidic anode, where the $CO_2$ is released with the electrochemically produced oxygen gas (Fig. 1a). This reaction necessitates a second $CO_2$ capture step to recycle the $CO_2$ from the anode gas, an additional energy expense that would not be required with a BPM or CEM electrolyser (Fig. 1b). Although there may be an additional balance of plant cost associated with recycling $CO_2$ from the anode outlet, the selectivity and energy efficiency — unparalleled in PEM or BPM systems — may outweigh this penalty. Learnings from analogous water electrolysis systems show that the cost of electrolytic fuel production is highly sensitive to electricity consumption or energy efficiency[9]; however, a detailed technoeconomic analysis should be performed to confirm this is the case for the $CO_2$ reduction reaction ($CO_2$RR). Further, alternative anodic reactions could be explored that have both liquid-phase reactants and products (for example, glycerol oxidation) and the $CO_2$ could simply be separated by phase rather than a capture unit.

Zero-gap $CO_2$RR reactors containing AEMs have demonstrated stable, high efficiencies (that is, selectivities >90% and cell voltages

[1]Department of Chemical and Biological Engineering, The University of British Columbia, Vancouver, British Columbia, Canada. [2]Department of Mechanical and Industrial Engineering, University of Toronto, Toronto, Ontario, Canada. [3]Department of Chemistry, Simon Fraser University, Burnaby, British Columbia, Canada. [4]Department of Chemical and Biomolecular Engineering, Vanderbilt University, Nashville, TN, USA. [5]Xergy Inc, Harrington, DE, USA. [6]Department of Materials Science and Engineering, The Pennsylvania State University, University Park, PA, USA. [7]Department of Chemistry and Chemical Biology, Rensselaer Polytechnic Institute, Troy, NY, USA. [8]Department of Electrical and Computer Engineering, University of Toronto, Toronto, Ontario, Canada. [9]Department of Chemistry, The University of British Columbia, Vancouver, British Columbia, Canada. [10]Stewart Blusson Quantum Matter Institute, The University of British Columbia, Vancouver, British Columbia, Canada. [11]Canadian Institute for Advanced Research (CIFAR), Toronto, Ontario, Canada. [12]These authors contributed equally: Danielle Salvatore, Christine Gabardo, Angelica Reyes, Colin O'Brien. ✉e-mail: cberling@chem.ubc.ca

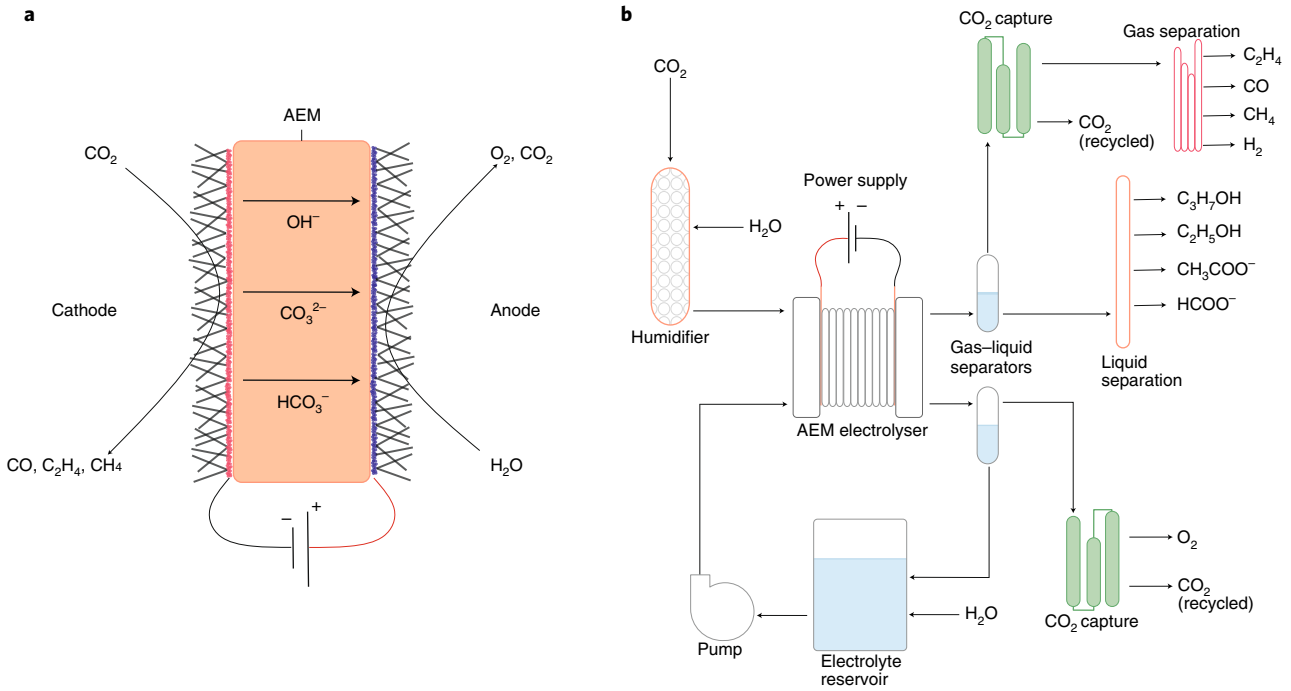


**Fig. 1 | AEM $CO_2$ electrolyser configuration and balance of plant. a**, A schematic of a $CO_2$ electrolyser. **b**, A process diagram showing the required balance of plant for a large-scale AEM electrolyser.

<3 V for >100 h) at high current densities (>200 mA cm$^{-2}$). In an AEM, positively charged functional groups on the polymer chain facilitate anion transport from the cathode to the anode, enabling the $CO_2$RR to occur in a basic environment due to the generation of hydroxide. AEM reactors may be more suitable for $CO_2$ reduction than CEM and reverse-bias BPM systems because a basic environment decreases the thermodynamic driving force for the competing hydrogen evolution reaction by decreasing the concentration of $H^+$ at the catalyst surface. Forward-bias BPM systems also enable a basic environment for the $CO_2$RR, but have demonstrated limited stability due to the delamination of the two membranes[10]. Silver, gold and copper heterogeneous catalysts, as well as molecular metal porphyrins, deposited on GDEs have been used in these AEM-based zero-gap reactor configurations for high conversion efficiencies to CO and multicarbon products (for example, $C_2H_4$, $C_2H_5OH$, $CH_3COO^-$)[5,11–13].

The efficiency of ion transport processes in membranes has been examined extensively in the context of water electrolysis[14], but far less so in $CO_2$RR. The lack of understanding of how membrane properties affect $CO_2$RR efficiency and selectivity motivates the need to explore these relationships[15]. Here we discuss AEMs in zero-gap reactors. We highlight desired properties of AEMs for the $CO_2$RR, review current state-of-art materials and propose key areas for future research.

## Principles of AEMs for $CO_2$ reduction

An ideal AEM conducts $OH^-$ at high rates from the cathode to the anode. AEMs contain hydrophilic cation groups that are anchored as side chains or directly incorporated into the hydrophobic polymer backbone[16]. There exist several different AEM structures that are reviewed comprehensively elsewhere[17–21]. Here we focus on those most relevant to the $CO_2$RR[5,22].

The transport of anions and water through dense AEMs are enabled by water-filled hydrated ionic domains in the polymer matrix. While the mechanism of anion transport through AEMs is still debated, there are two dominant transport mechanisms: vehicular transport and Grotthuss hopping (Fig. 2)[23,24].

Grotthuss hopping is the propagation of $OH^-$ through the hydrogen-bond network of water molecules by the formation and cleavage of covalent bonds with the neighbouring molecules[24]. Vehicular transport includes both the concentration gradient-driven diffusion and electromigration mechanisms. Diffusion occurs in response to a concentration gradient, and electromigration of charged species occurs in response to an electrical potential gradient. While the driving forces for diffusion and electromigration are different, both mechanisms depend on the diffusion coefficient of ions transported through the membrane[25]. The structure and water content of the AEM influence the diffusion coefficient of ions. Both hopping and vehicular transport mechanisms require free, also known as unbound, water within the membrane (that is, hydrated domains or water pools with limited hydration interactions with the backbone and side chains). In a membrane with low hydration levels, the solvation of the ionic groups does not facilitate unbound water. In that case, the hopping mechanism is not active, vehicular transport is curtailed and the ionic conductivity of the membrane will be low[23,24]. In a highly hydrated membrane, the ionic domains are water filled and typically enlarged. Ion transport will occur through the free water (that is, Grotthuss hopping), and the ionic conductivity of the membrane will be high[23,24]. Excess water can also decrease the overall material conductivity, wherein the membrane swells to the point where ion mobility is maximum but the concentration of ions decreases due to dilution, and conductivity decreases with further hydration[26].

The management of water has emerged as an important factor influencing the performance of the $CO_2$RR, as it is for AEM fuel cells[27,28]. Water is a reactant in the conversion of $CO_2$, but excess water will block $CO_2$ diffusion to the catalyst, and the reaction will favour the hydrogen evolution reaction. Water can be delivered to the $CO_2$ catalyst in a zero-gap reactor from a humidified gas stream and/or from the membrane. Diffusion, electro-osmotic drag and convection describe the different modes of transport of water across the membrane (Fig. 2)[29]. Water can diffuse from the anode to the cathode in response to a concentration gradient between the aqueous anode environment and the gas-fed cathode. Water is also

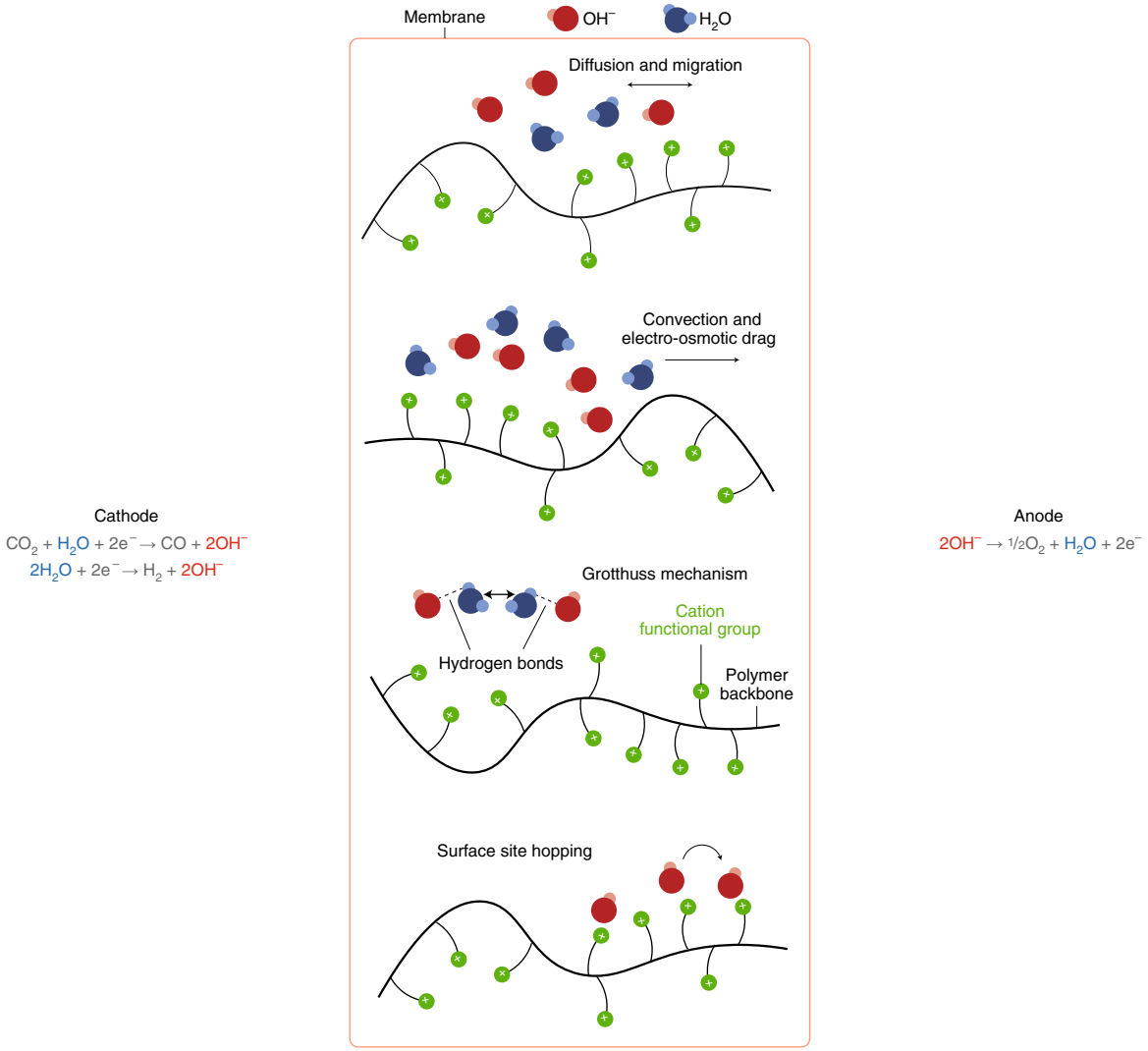


**Fig. 2 | Mechanisms of anion and water transport in AEMs.** Possible combinations of transport mechanisms for anions and water in the AEM.

drawn from the cathode to the anode through electro-osmotic drag as solvated anions migrate towards the anode[30]. Back convection of water from the cathode to the anode is driven by the increased liquid pressure associated with using hydrophobic cathode GDEs[31] and by the higher water permeation through thinner membranes[32]. The uncharged liquid $CO_2$RR products follow the same transport mechanisms as water, whereas the charged liquid $CO_2$RR products follow the anionic transport mechanisms. The net amount of water transported to the electrocatalyst following each of these mechanisms depends on the microstructure and chemical properties of the membrane, as well as the operating conditions. Thus, a holistic view of materials performance, cell construction and operating conditions is needed to achieve the water balance required for high-performance $CO_2$RR.

The properties of commercially available and experimental AEMs have been reported in the context of fuel-cell and water electrolyser conditions, but there are currently no protocols or metrics established for $CO_2$RR electrolysers. Ion exchange capacity (IEC) and the chemical composition of the membrane influence water uptake, mechanical strength, ion conductivity and water transport of the membrane. We highlight two key characterization metrics — ion conductivity and water uptake measurements — that are critical to the performance and may impact the chemical stability and long-term device performance of AEMs for $CO_2$RR.

Ionic conductivity is an important contributor to the full cell voltage of $CO_2$ electrolysers. Through-plane conductivity is more relevant than in-plane conductivity because anion transport occurs predominantly through the thickness of the membrane. However, the accurate measurement of through-plane conductivity using a.c. impedance is challenging and requires a specialized cell and a correction for non-membrane resistances (for example, the surface impedance between the membrane and electrodes). A simpler two-electrode set-up measuring anion conductivity ($\sigma$ in $S\,cm^{-1}$, equation (1)) in the in-plane direction is commonly employed with the assumption that conductivity in an AEM is isotropic[33]. Here conductivity is calculated from the resistance of the membrane ($R_{mem}$ in Ω) obtained from the high-frequency data in the Nyquist plot, the cross-sectional membrane area ($A$ = width of the sample × the membrane thickness, in units of $cm^2$) and the distance between the two working electrodes ($L$ in units of cm):

$$\sigma = \frac{L}{R_{mem} \times A} \quad (1)$$

Recently, a technique for accurate measurement of hydroxide conductivity was reported that involves measuring the conductivity during water splitting, wherein hydroxide ions produced at the cathode purge the other anions[34]. However, measuring the $OH^-$

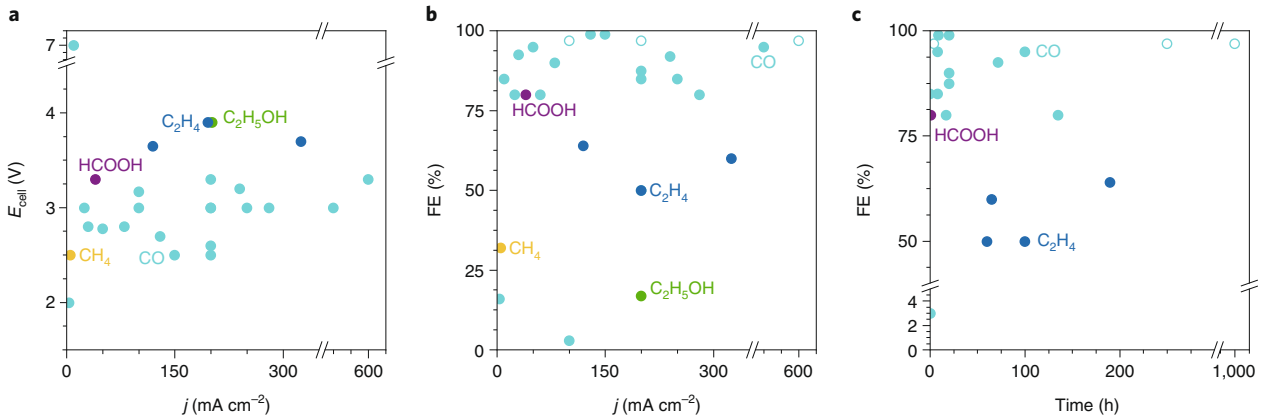


**Fig. 3 | Performance of AEM-based gas-phase $CO_2$ electrolysers. a**,**b**, Cell voltage (**a**) and Faradaic efficiency (**b**) versus current density (*j*) for carbon monoxide (CO), formic acid (HCOOH), methane ($CH_4$), ethylene ($C_2H_4$) and ethanol ($C_2H_5OH$). **c**, Faradaic efficiency versus operating time for carbon monoxide, formic acid and ethylene. Hollow circle symbols indicate selectivity instead of Faradaic efficiency. The data constituting these plots are based on previous reports that use AEMs in zero-gap electrolysers fed with gaseous $CO_2$, and can be found in the Source Data file[5,6,11,13,22,35,43–45,47,52–55,60,63,81–90].

conductivity is not relevant in $CO_2$ electrolysers because the primary charge carrier in AEMs is $CO_3^{2-}$ based on the high pH (>11) at the cathode[10,35,36]. The $CO_3^{2-}$ conductivity of AEMs should therefore be measured in the future to benchmark the performance of newly synthesized AEMs for $CO_2$ electrolysers. While Nafion has been widely used as the benchmark membrane in PEM devices, so far there is no analogous benchmark AEM that can serve for comparison with newly developed AEM materials.

High-ionic-conductivity membranes (>60 mS cm$^{-1}$) are enabled by high IEC, which is defined as the number of exchangeable cation groups per dry weight of polymer (milliequivalent per gram). This allows a continuous network of water channels upon hydration without excessive water swelling. IEC can be measured using titration (for example, Mohr method, acid/base), an ion-selective electrode and spectroscopy (for example, ultraviolet–visible, NMR); however, there are variations among IECs measured using each procedure, and the IEC depends on the chemical composition of the membrane[18].

Water in the AEM is essential for anion transport through the AEM, but high water content can cause the membrane to swell excessively, compromising mechanical integrity and inducing stresses[37]. The water content of the AEM is related to the water uptake property, which is the percentage increase in the mass of the AEM when it is fully equilibrated in liquid or water vapour relative to a dry state[38]. This property is also a measure of the free volume in the polymer matrix available for water and ion transport. Considering ionic conductivity, IEC and water uptake together, the water uptake of the membrane is a key parameter that ultimately determines membrane performance, as described in a number of papers that provide a fundamental view of how these water-absorbing solid-state electrolytes behave[39–42].

## Remaining challenges for implementation of AEMs in $CO_2$ electrolysers

Early reports of AEM-based $CO_2$ electrolysers used membranes that were originally developed for electrochemical applications under mild pH conditions such as electrodialysis for desalination, waste-water treatment and mineral refining[6,43–45]. However, major operational challenges have been encountered when using these membranes in AEM-based $CO_2$ electrolysers. First, product and reactant crossover to the anode is a prominant issue. Negatively charged $CO_2$RR products (for example, $HCOO^-$) are readily transported across the positively charged AEM, while neutral products (for example, ethanol) are also able to cross over through sorption into and subsequent diffusion through the membrane[46]. Moreover, the reaction between the $CO_2$ feed and $CO_2$RR-generated $OH^-$ produces $HCO_3^-$ and $CO_3^{2-}$, which reduces the amount of free $CO_2$ available to the catalyst. The generated $HCO_3^-$ and $CO_3^{2-}$ also diffuse through the AEM to the anode electrolyte and are converted back to a substantial volume of $CO_2$, often exceeding the amount of $CO_2$ converted to the target product (60% of total $CO_2$ is neutralized)[35].

Water management is crucial for AEM-based zero-gap reactors to balance water as a proton source for $CO_2$RR and prevent flooding[47,48]. Thin (20 µm), low-water-uptake (~40%) AEMs have been shown to mitigate cathode flooding and improve $CO_2$RR performance. Cathode flooding is also linked to salt precipitation at the cathode[49,50]. Water is a medium for the transport of $K^+$ from the anode electrolyte (which is often KOH or $KHCO_3$) to the cathode, thus reacting with $CO_2$ to form crystals (for example, $KHCO_3$, $K_2CO_3$) that block the pores of the GDE[5,48]. The use of pure water at the anode reduces $KHCO_3$ and $K_2CO_3$ crystal formation at the expense of ionic conductivity and cell potential.

Another major operational issue is the mechanical and chemical stability of commercial AEMs. A commercially available electrodialysis AEM that is chemically stable up to a pH of 10 has been used previously. However, AEM-based $CO_2$ electrolysers operate at a higher pH (>11) than electrodialysis systems because $OH^-$ ions are electrochemically generated at the cathode[13,35,48]. Although there is buffering at the cathode in the presence of $CO_2$, pH at the cathode increases largely at high current densities. This incompatibility between the operational requirements of a $CO_2$ electrolyser and the chemical properties of many existing AEMs is a root cause of limited cell stability (Fig. 3). Finally, zero-gap $CO_2$ electrolysers tend to suffer from low energy efficiencies. There are very few examples of cells that achieve high current densities >200 mA cm$^{-2}$ at cell voltages <3 V (Fig. 3). The high measured cell voltages are largely due to interfacial and ohmic losses in AEM zero-gap $CO_2$ electrolysers[51]. Improvements in $CO_2$RR performance have been realized with the recent developments of AEMs tailored for gas-phase $CO_2$ electrolysis experiments, but there remains room for membrane innovations to bring these systems closer to commercial viability.

Sustainion, an *N*-methylimidazolium-functionalized styrene polymer (Fig. 4a), is an AEM designed for gas-fed $CO_2$ electrolysers in the presence of electrolyte (10 mM $KHCO_3$)[52]. This membrane features a high $OH^-$ conductivity (102 mS cm$^{-1}$ at 80 °C in 1 M KOH), possesses a high IEC (2.52 meq g$^{-1}$), displays substantial water uptake (80%) and is thin (50 µm)[53]. The high conductivity of this membrane was maintained in a $CO_2$ electrolyser with a humidified

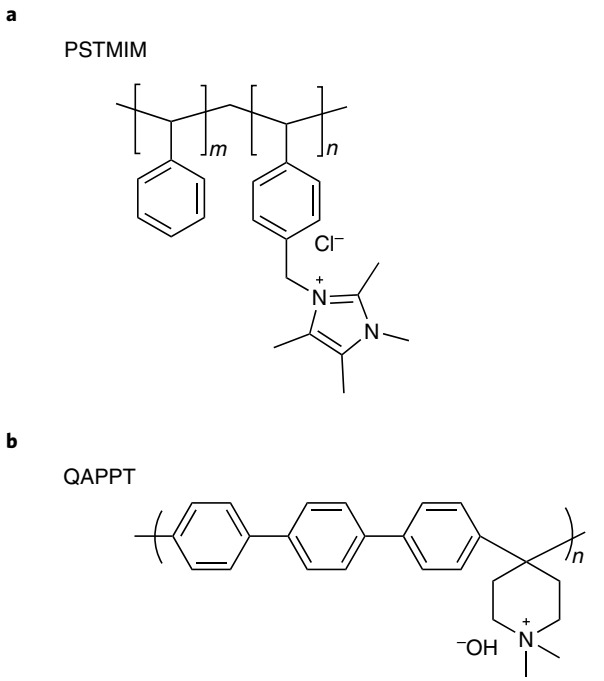


**Fig. 4 | Structures of AEMs used in $CO_2$ electrolysers. a**,**b**, Chemical structures of polystyrene tetramethyl imidazolium chloride (PSTMIM) commercialized as Sustainion (**a**) and QAPPT (**b**) AEMs.

gaseous $CO_2$ feed and a circulating aqueous anolyte of 10 mM $KHCO_3$ at the anode, while reaching commercially relevant current densities (200 mA cm$^{-2}$) and sustaining >95% CO selectivity at 3 V for 3,800 h. Many studies have since followed this approach in gas-fed $CO_2$ electrolysers[11,13,54,55]. However, Sustainion is prone to crossover of $CO_2$RR products (for example, ethanol), particularly at the high current densities relevant to commercial operation[13].

A quaternary ammonium poly(*N*-methyl-piperidine-co-*p*-terphenyl) (QAPPT) was also introduced as another candidate AEM material for gas-fed $CO_2$ electrolysers (Fig. 4b)[22]. QAPPT exhibits a higher $OH^-$ conductivity (137 mS cm$^{-1}$ at 80 °C) and is more chemically stable in high pH solutions than Sustainion at elevated temperatures (>80 °C) because the polymer is made of aryl ether-free polymer backbone and a long alkyl-tethered ammonium head group[21,22,56,57]. The high conductivity of QAPPT eliminates the need to humidify the $CO_2$ feed or to use an ionically conductive anolyte (that is, the authors used pure water at the anode). With an operating cell temperature of 60 °C, the QAPPT-containing $CO_2$ electrolyser demonstrated the highest current density reported so far (500 mA cm$^{-2}$) with an Faradaic efficiency for CO ($FE_{CO}$) of >90% and a cell voltage ($E_{cell}$) of 3 V. This result motivates further research on incorporating QAPPT for use in $C_{2+}$-producing systems, and the potential to address other persistent challenges for previous AEMs in $CO_2$ electrolysers. In a recent study, this piperidinium-based AEM has been reported to have an amorphous structure with no detectable ionic group aggregation[58].

These two case studies illustrate the importance of fabricating advanced AEMs with characteristics that match the requirements of $CO_2$ electrolysers. While commercially available AEMs suffer from low $OH^-$ conductivities and poor stabilities in a high pH range (10–15), Sustainion and QAPPT exhibit high ionic conductivities and alkali stabilities compatible with $CO_2$ electrolysis. Table 1 lists the desired properties for an AEM used in a zero-gap $CO_2$RR reactor. The IECs and thicknesses of both Sustainion (IEC, 2.52 meq g$^{-1}$; thickness, 50 μm) and QAPPT (IEC, 2.65 meq g$^{-1}$; thickness, 25 μm) align with the desired properties for AEMs in $CO_2$ electrolysers as highlighted in Table 1. As in the case of QAPPT, it is important for AEMs to maintain chemical and mechanical integrity at higher operating cell temperatures (up to 80 °C) and with added electrolyte, where $CO_2$RR kinetics are improved[22]. It is encouraging to see some high-performance AEMs becoming available commercially. For example, Aemion (IEC, 2.1 meq g$^{-1}$; thickness, 60 μm) is an emerging AEM that exhibits a higher chemical resistance to ethanol compared with Sustainion[13]. Recently commercialized polyaromatic AEM Orion has also demonstrated excellent performances in hydrogen fuel cells and water electrolysis[21].

**Table 1 | Desired properties for AEMs for $CO_2$RR**

| | Parameter | Required specification |
|---|---|---|
| Transport properties | Area specific resistance | <0.1 Ω cm$^2$ (<0.02 Ω cm$^2$ ideal) |
| | Through-plane $OH^-$ conductivity | 60–100 mS cm$^{-1}$ |
| | Thickness | 5–100 μm |
| | IEC | >1.5 meq g$^{-1}$ |
| Mechanical properties | Elongation at break | $\varepsilon > 1.5$ |
| | Young's modulus | $E \approx 0.25$ GPa |
| | Ultimate tensile strength | $U \approx 20$ MPa |
| | Water uptake | 50–80% |
| | In-plane swelling | <15% (ideally <10%) |
| Chemical properties | pH range | 10–14 |
| | Temperature | 20–80 °C |
| | Stability | Insoluble in 10 wt% alcohol |
| | Crossover | Minimal gas/liquid product crossover (<0.2%) |
| Testing conditions | Time | >1,000 h |
| | Voltage | <3 V cell voltage |
| | Current density | 200–2,000 mA cm$^{-2}$ |

## Binders for $CO_2$RR AEM electrolyser catalyst layers

Binders are often added to catalyst layers to improve the mechanical durability and prevent catalyst delamination from the GDE. Using ionomers as binders enhances the ion conductivity and provides access for the reactants, $CO_2$ and water, and facilitates removal of anions to and from the catalyst. At present, anion exchange ionomers, cation exchange ionomers and polytetrafluoroethylene (PTFE) are all commonly used as binders in the cathode and anode catalyst layers of AEM zero-gap reactors.

Anion exchange ionomer binders allow for the best integration of ion transport with the membrane, creating a more cohesive ion transport path that has allowed for cell voltages <3 V (refs. [5,22,59]). The commercially available anion exchange ionomers, based on similar polymers as the corresponding AEMs, suffer from many of the same shortcomings: limited commercially available options with high pH resistance, mechanical instability and water accumulation. Cation exchange ionomer binders have shown to increase the mass transport of $CO_2$ along the hydrophobic backbone, which allows for a larger catalytically active surface area and leads to an increase in the current density[60–62]. This phenomenon has also allowed for cell voltages <3 V in an AEM zero-gap reactor[55,63]. These cation exchange ionomers have many more commercially available options that are chemically and mechanically stable. A binder developed specifically

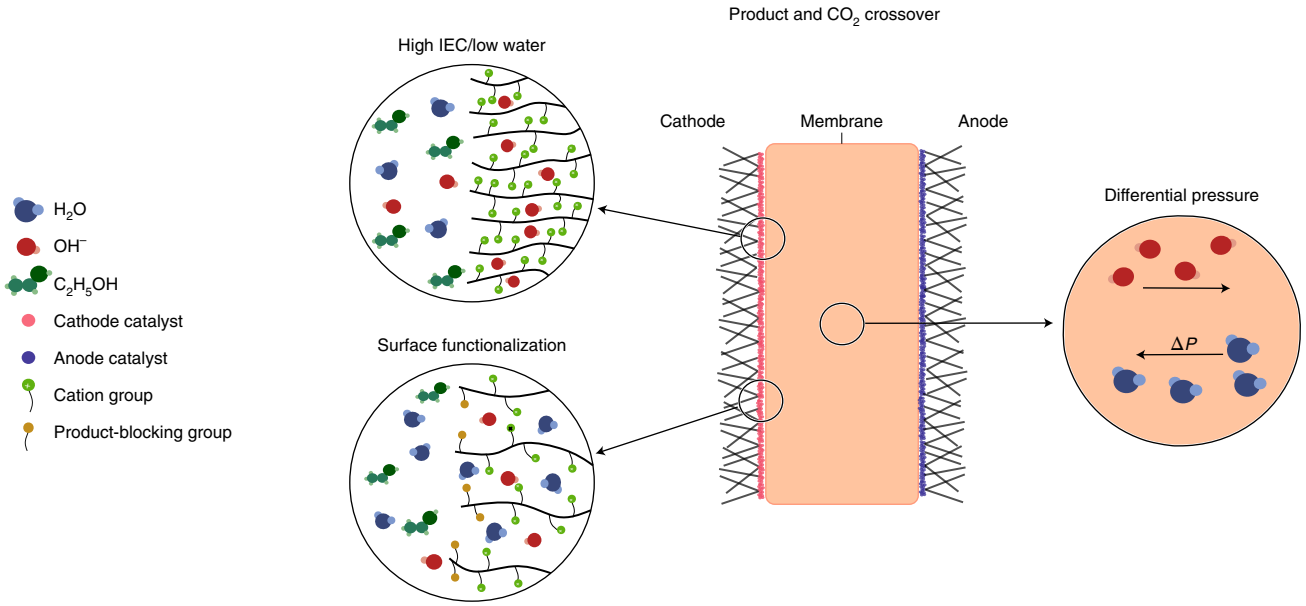


**Fig. 5 | Strategies to mitigate product and $CO_2$ crossover in AEMs.** Product and $CO_2$ crossover can be mitigated by fabricating AEMs that show high IEC and low water uptake, by functionalizing the surface and by inducing a differential pressure across the AEM.

for $CO_2$RR would combine the ionic conductivity of anion exchange binders with the mass transport of cation exchange binders, while meeting all of the requirements outlined in Table 1.

## Future direction on design of AEMs for $CO_2$ reduction

Designing new AEMs specific for $CO_2$RR cells is integral to realizing a commercially viable zero-gap $CO_2$ reactor. The engineering of effective $CO_2$RR membranes should focus on reducing product and $CO_2$ crossover, increasing chemical and mechanical stability, and reducing interfacial and other resistive losses in the zero-gap reactors. While membrane design and operational strategies can be translated from allied electrochemical technologies, new membrane materials and morphologies will need to be developed to address the distinct challenges for $CO_2$RR and meet the desired properties listed in Table 1. Here we outline some proposed approaches that could be applied to zero-gap AEM reactors for $CO_2$RR (Figs. 5–7).

**Product and $CO_2$ crossover.** The water uptake of the membrane is a key parameter that can modulate the undesired crossover of $CO_2$RR products through the AEM[41,42,64]. The transport of neutral $CO_2$ reduction product species through the membrane is directly related to the membrane water volume fraction because the diffusion coefficient is much higher in water-filled ionic domains. To decrease neutral liquid product crossover, AEMs can be tailored to have low water uptake (Fig. 5), where water (that is, the proton source) for the $CO_2$RR must be supplied by the humidification of the $CO_2$ stream. In a membrane with low water uptake, there will generally be less mixing of the liquid products with water and less drag to the anode. Despite the lack of free water in the membrane, a high IEC could maintain high anion conductivity. Moreover, a membrane and a cathode ionomer engineered to have a low water uptake and high IEC could aid in reducing $HCO_3^-/CO_3^{2-}$ crossover through the membrane by limiting the amount of aqueous $CO_2$ present within the membrane, and therefore reducing the reaction with $OH^-$. Chemically modifying the surface of the AEM with functional groups could also selectively trap or repel liquid products from the membrane while allowing for water and ions to be transported. Functional groups that change the size of the free volume elements within the membrane (that is, sterically hinder product crossover) or functional groups that can chemically interact with the product (for example, with the alcohol groups on ethanol) could reduce crossover. However, to incorporate product-blocking functional groups on the surface of the membrane, ion-conducting functional groups will be displaced. It is therefore important to minimize the number of replaced ion-conducting functional groups to maintain high anion conductivity. Solid additive materials (for example, silica nanoparticles and carbon nanotubes) have also been incorporated into direct methanol fuel-cell membranes to prevent methanol crossover and a similar approach should be pursued for the $CO_2$RR[65,66].

Another strategy to mitigate crossover is to operate the zero-gap electrolyser with a differential pressure between the cathode and anode. A higher pressure at the anode can decrease water convection from the cathode to anode, and thus, reduce product transport through convecting drag. Under these high-pressure differential conditions, the AEM would have to be designed to remain mechanically stable and the cathode would need to be engineered to prevent flooding.

**Chemical and mechanical stability.** The lifetime of $CO_2$RR electrolysers is currently limited by the degradation of the AEMs — a coupled chemical and mechanical process (Fig. 6). Because AEMs typically require a high IEC (for example, $>2.0\,meq\,g^{-1}$) to achieve sufficient anion conductivity, they tend to swell and are mechanically weaker than Nafion (that is, AEMs exhibit lower tensile strength and elongation at break). The hygroscopic nature of an AEM results in a high water uptake to provide the required water to the cathode from the anolyte. Chemical crosslinking, through the creation of ionic or covalent bonds between different chains of polymer backbones, can provide high-dimensional stability for membranes and improve the tensile strength[67–69]. Further, mechanical reinforcement can be incorporated through the use of polymer blends[70], co-deposition of ionomers with composite nanofibre mats[71] or by casting the ionomers over high-strength porous mesh or scaffolds[69]. These strategies, coupled with robust chemical stability of the material, can lead to long-lived $CO_2$RR reactors.

The electrochemical generation of $OH^-$ ions at the cathode from $CO_2$RR necessitates AEMs that are chemically stable at high pH (up to 14)[72]. Under this highly basic environment, the polymer backbone[73] and cation headgroups[74] are susceptible to attack by the

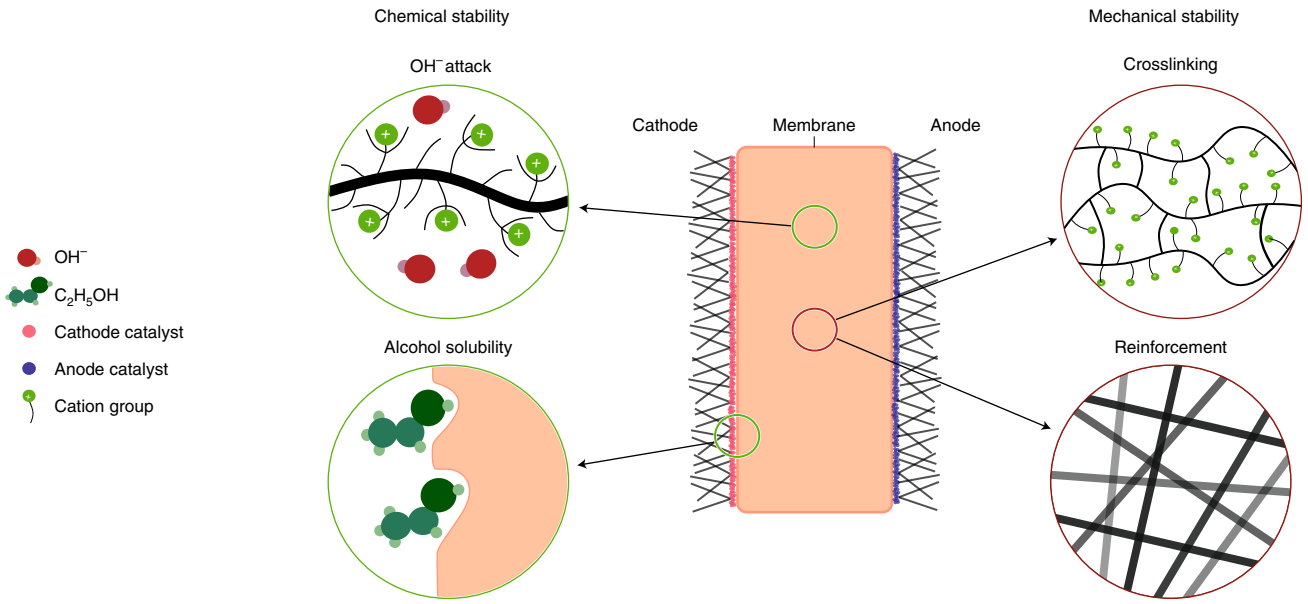


**Fig. 6 | Strategies to improve $CO_2$RR AEM chemical and mechanical stability.** Developing AEMs that are crosslinked[67–69] or reinforced[69–71] are strategies to improve mechanical stability, while AEM designs that are resistant to $OH^-$ attack[73–75] and are insoluble in alcohols are important for chemical stability.

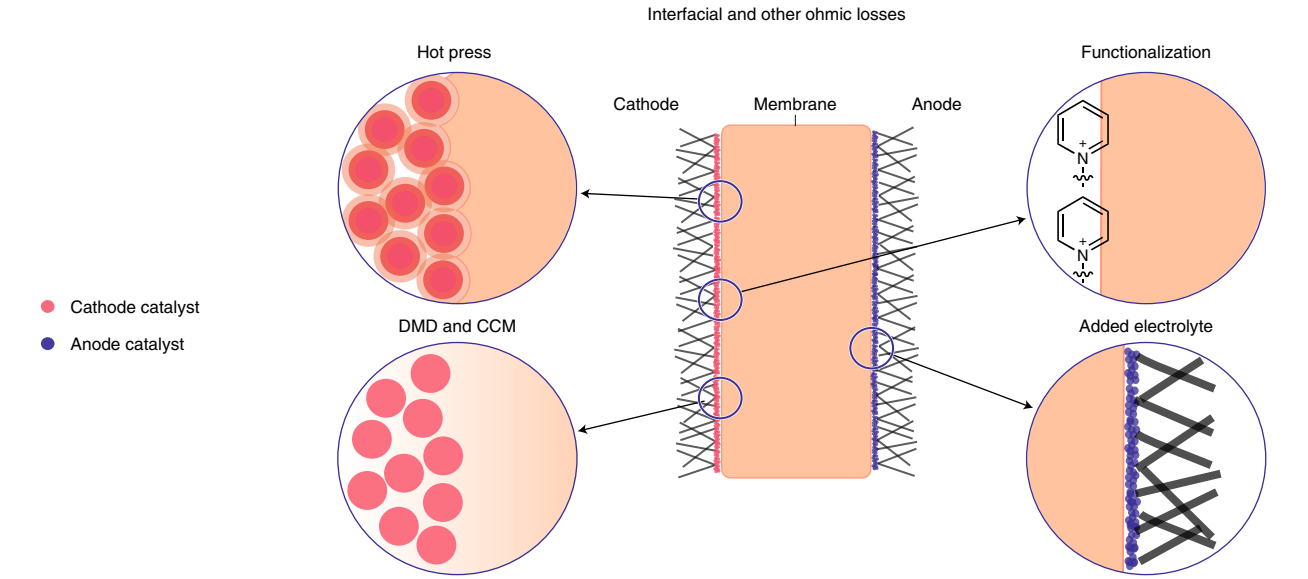


**Fig. 7 | Strategies to improve $CO_2$RR AEM interfaces and energy efficiency.** Interfacial resistances associated with AEM interfaces can be minimized by using the hot-press technique, DMD or a CCM[76,77]. Adding dilute electrolyte at the anode[78] or functionalizing the surface of AEMs with bulk ionic groups[79,80] are important in improving energetic efficiencies.

$OH^-$ ions that leads to polymer backbone cleavage and nucleophilic displacement or elimination reactions, respectively. The presence of hydroxide combined with oxygen can generate organic peroxides and hydroperoxides, through radical reactions, leading to the oxidation of the polymer backbone and chain scission[75]. This chemical attack ultimately leads to reduced anion transport and a loss of membrane mechanical integrity. Innovative polymer synthesis strategies to enhance chemical stability by protecting both of these susceptible areas (for example, the shielding of backbones through steric hindrance or making more chemically resistant functional groups against intermediate oxygen species) are critical for long-term $CO_2$RR device stability (Fig. 6)[21]. An additional consideration is to create AEMs that remain robust in the presence of all $CO_2$RR products of interest, and particularly ethanol and higher alcohols. Anion exchange ionomers, which serve as binders at the catalyst layer, are often soluble in alcohol solvents for convenient electrode fabrication. However, AEMs should be designed to be insoluble in these solvent systems since concentrated alcohols (ethanol, *n*-propanol) can be products of the $CO_2$RR. Next-generation AEMs should be engineered to remain chemically and mechanically robust under $CO_2$ electrolysis conditions.

**Interfacial and ohmic losses.** Most membrane electrode assemblies for zero-gap $CO_2$RR devices are fabricated by manually compressing a hydrated membrane between a cathode and anode. In these configurations, the cathode and anode catalysts may not have the

requisite intimate contact needed for efficient ion transfer from the electrodes to the membrane. Many similar electrochemical technologies have overcome these interfacial losses by applying heat and pressure through hot pressing, fabricating catalyst-coated membranes (CCMs), and direct membrane deposition (DMD)[76,77], physically depositing the ionomers that form the membrane directly on the gas diffusion cathode (Fig. 7). These techniques have not yet been widely tested in $CO_2$RR devices primarily because most commercially available AEMs are fragile, the catalyst layer cracks and swells when coated directly on the membrane, and there is a limited library of ionomers available to directly deposit on GDEs. Increasing the processability of commercially available AEMs would greatly reduce the interfacial losses in zero-gap $CO_2$RR systems, thus improving energy efficiency.

Due to these difficulties with processing anion exchange ionomers, many recent AEM water electrolysers use dilute $K_2CO_3$ electrolytes to increase the ionic conductivity of the anode–membrane interface and improve the stability by reducing the hydroxide concentration in the membrane[78]. However, if the AEM is not adequately selective for anions, the transport of $K^+$ will slowly increase the evolution of $CO_2$ from the carbonate anolyte, reducing the conductivity of the anolyte over time. Similar to tuning the catholyte composition (cations, anions, pH, organic additives and so on) in liquid-filled reactors, the surface or bulk functional groups of membranes can be tuned to control the local reaction environment at the catalyst to improve the energetic efficiency of the $CO_2$RR[79]. For example, pyridinium-based functional groups incorporated at the membrane surface could modulate pH and improve $CO_2$RR selectivity (Fig. 7)[80]. Improving the energy efficiency of $CO_2$RR electrolysers will be contingent on designing AEMs that can be integrated with membrane electrode assembly best practices and are precisely tuned to create local environments at the catalysts that favour $CO_2$RR.

## Conclusions

The relevance of near-ambient-temperature $CO_2$RR electrolysis hinges on the advancement of anion exchange membranes. AEMs need to be specifically tailored for the $CO_2$RR because the reactants, products and operating conditions differ from other electrolyser technologies that make use of them. The next generation of AEMs should address these challenges while targeting the metrics listed in Table 1. Satisfying these requirements is a challenge — altering one membrane property will most often alter other membrane properties. It will be important to overcome these trade-offs to design the best possible membrane tailored for each $CO_2$RR application (gas product, liquid product, $CO_2$ or CO as a reactant).

Received: 10 February 2020; Accepted: 7 December 2020;
Published online: 11 February 2021

## References

1. Weekes, D. M., Salvatore, D. A., Reyes, A., Huang, A. & Berlinguette, C. P. Electrolytic $CO_2$ reduction in a flow cell. *Acc. Chem. Res.* **51**, 910–918 (2018).
2. Jouny, M., Luc, W. & Jiao, F. General techno-economic analysis of $CO_2$ electrolysis systems. *Ind. Eng. Chem. Res.* **57**, 2165–2177 (2018).
3. Mehta, V. & Cooper, J. S. Review and analysis of PEM fuel cell design and manufacturing. *J. Power Sources* **114**, 32–53 (2003).
4. Millet, P. et al. PEM water electrolyzers: from electrocatalysis to stack development. *Int. J. Hydrogen Energy* **35**, 5043–5052 (2010).
5. Kutz, R. B. et al. Sustainion imidazolium-functionalized polymers for carbon dioxide electrolysis. *Energy Technol.* **5**, 929–936 (2017).
**Research paper that describes a Sustainion AEM $CO_2$ electrolyser for CO production and boasts 1,000 h reaction stability**.
6. Delacourt, C., Ridgway, P. L., Kerr, J. B. & Newman, J. Design of an electrochemical cell making syngas ($CO+H_2$) from $CO_2$ and $H_2O$ reduction at room temperature. *J. Electrochem. Soc.* **155**, B42–B49 (2008).
7. Salvatore, D. A. et al. Electrolysis of gaseous $CO_2$ to CO in a flow cell with a bipolar membrane. *ACS Energy Lett.* **3**, 149–154 (2018).
8. Herranz, J., Patru, A., Fabbri, E. & Schmidt, T. J. Co-electrolysis of $CO_2$ and $H_2O$: from electrode reactions to cell level development. *Curr. Opin. Electrochem*. https://doi.org/10.1016/j.coelec.2020.05.004 (2020).
9. Ainscough, C., Peterson, D. & Miller, E. *DOE Hydrogen And Fuel Cells Program Record 14004* Technical Report 7 (US DOE, 2014).
10. Pătru, A., Binninger, T., Pribyl, B. & Schmidt, T. J. Design principles of bipolar electrochemical co-electrolysis cells for efficient reduction of carbon dioxide from gas phase at low temperature. *J. Electrochem. Soc.* **166**, F34–F43 (2019).
11. Ren, S. et al. Molecular electrocatalysts can mediate fast, selective $CO_2$ reduction in a flow cell. *Science* **365**, 367–369 (2019).
12. Wang, M. et al. $CO_2$ electrochemical catalytic reduction with a highly active cobalt phthalocyanine. *Nat. Commun.* **10**, 3602 (2019).
13. Gabardo, C. M. et al. Continuous carbon dioxide electroreduction to concentrated multi-carbon products using a membrane electrode assembly. *Joule* **3**, 2777–2791 (2019).
**Research paper that describes an AEM $CO_2$ electrolyser for producing $C_{2+}$ products, ethylene and concentrated ethanol, and discusses the challenges with product crossover**.
14. Oener, S. Z., Ardo, S. & Boettcher, S. W. Ionic processes in water electrolysis: the role of ion-selective membranes. *ACS Energy Lett.* **2**, 2625–2634 (2017).
15. Aeshala, L. M., Uppaluri, R. & Verma, A. Electrochemical conversion of $CO_2$ to fuels: tuning of the reaction zone using suitable functional groups in a solid polymer electrolyte. *Phys. Chem. Chem. Phys.* **16**, 17588–17594 (2014).
16. Merle, G., Wessling, M. & Nijmeijer, K. Anion exchange membranes for alkaline fuel cells: a review. *J. Membr. Sci.* **377**, 1–35 (2011).
17. Holdcroft, S. & Fan, J. Sterically-encumbered ionenes as hydroxide ion-conducting polymer membranes. *Curr. Opin. Electrochem.* **18**, 99–105 (2019).
18. Varcoe, J. R. et al. Anion-exchange membranes in electrochemical energy systems. *Energy Environ. Sci.* **7**, 3135–3191 (2014).
**Perspective paper that discusses the key concepts, misconceptions, technological and scientific limitations, and research priorities for anion exchange membranes in electrochemical devices**.
19. Ramaswamy, N. & Mukerjee, S. Alkaline anion-exchange membrane fuel cells: challenges in electrocatalysis and interfacial charge transfer. *Chem. Rev.* **119**, 11945–11979 (2019).
20. Gottesfeld, S. et al. Anion exchange membrane fuel cells: current status and remaining challenges. *J. Power Sources* **375**, 170–184 (2018).
21. Noh, S., Jeon, J. Y., Adhikari, S., Kim, Y. S. & Bae, C. Molecular engineering of hydroxide conducting polymers for anion exchange membranes in electrochemical energy conversion technology. *Acc. Chem. Res.* **52**, 2745–2755 (2019).
22. Yin, Z. et al. An alkaline polymer electrolyte $CO_2$ electrolyzer operated with pure water. *Energy Environ. Sci.* **12**, 2455–2246 (2019).
**Research paper that describes a QAPPT AEM $CO_2$ electrolyser for CO production that uses pure water as an electrolyte**.
23. Zawodzinski, T. A., Neeman, M., Sillerud, L. O. & Gottesfeld, S. Determination of water diffusion coefficients in perfluorosulfonate ionomeric membranes. *J. Phys. Chem.* **95**, 6040–6044 (1991).
24. Tuckerman, M. E., Marx, D. & Parrinello, M. The nature and transport mechanism of hydrated hydroxide ions in aqueous solution. *Nature* **417**, 925–929 (2002).
25. Kamcev, J. & Freeman, B. D. Charged polymer membranes for environmental/energy applications. *Annu. Rev. Chem. Biomol. Eng.* **7**, 111–133 (2016).
26. Lee, K. M., Wycisk, R., Litt, M. & Pintauro, P. N. Alkaline fuel cell membranes from xylylene block ionenes. *J. Membr. Sci.* **383**, 254–261 (2011).
27. Zheng, Y. et al. Water uptake study of anion exchange membranes. *Macromolecules* **51**, 3264–3278 (2018).
28. Mangiagli, P. M., Ewing, C. S., Xu, K., Wang, Q. & Hickner, M. A. Dynamic water uptake of flexible ion-containing polymer networks. *Fuel Cells* **9**, 432–438 (2009).
29. Li, Y. S., Zhao, T. S. & Chen, R. Cathode flooding behaviour in alkaline direct ethanol fuel cells. *J. Power Sources* **196**, 133–139 (2011).
30. Zawodzinski, T. A., Davey, J., Valerio, J. & Gottesfeld, S. The water content dependence of electro-osmotic drag in proton-conducting polymer electrolytes. *Electrochim. Acta* **40**, 297–302 (1995).
31. Xu, C. & Zhao, T. S. In situ measurements of water crossover through the membrane for direct methanol fuel cells. *J. Power Sources* **168**, 143–153 (2007).
32. Liu, F., Lu, G. & Wang, C.-Y. Low crossover of methanol and water through thin membranes in direct methanol fuel cells. *J. Electrochem. Soc.* **153**, A543–A553 (2006).
33. Zawodzinskijr, T., Springer, T., Uribe, F. & Gottesfeld, S. Characterization of polymer electrolytes for fuel cell applications. *Solid State Ion.* **60**, 199–211 (1993).
34. Ziv, N. & Dekel, D. R. A practical method for measuring the true hydroxide conductivity of anion exchange membranes. *Electrochem. Commun.* **88**, 109–113 (2018).

35. Larrazábal, G. O. et al. Analysis of mass flows and membrane cross-over in $CO_2$ reduction at high current densities in an MEA-type electrolyzer. *ACS Appl. Mater. Interfaces* **11**, 41281–41288 (2019).
**Research paper that analyses the mass balance in an AEM $CO_2$ electrolyser and discusses $CO_2$ crossover via carbonate formation.**
36. Lu, X. et al. In-situ observation of the pH gradient near the gas diffusion electrode of $CO_2$ reduction in alkaline electrolyte. *J. Am. Chem. Soc.* https://doi.org/10.1021/jacs.0c06779 (2020).
37. Pan, J. et al. High-performance alkaline polymer electrolyte for fuel cell applications. *Adv. Funct. Mater.* **20**, 312–319 (2010).
38. Thieu, L. M., Zhu, L., Korovich, A. G., Hickner, M. A. & Madsen, L. A. Multiscale tortuous diffusion in anion and cation exchange membranes. *Macromolecules* **52**, 24–35 (2019).
39. Disabb-Miller, M. L., Johnson, Z. D. & Hickner, M. A. Ion motion in anion and proton-conducting triblock copolymers. *Macromolecules* **46**, 949–956 (2013).
40. Kim, Y. S. & Pivovar, B. S. Moving beyond mass-based parameters for conductivity analysis of sulfonated polymers. *Annu. Rev. Chem. Biomol. Eng.* **1**, 123–148 (2010).
41. Dischinger, S. M., Gupta, S., Carter, B. M. & Miller, D. J. Transport of neutral and charged solutes in imidazolium-functionalized poly(phenylene oxide) membranes for artificial photosynthesis. *Ind. Eng. Chem. Res.* **59**, 5257–5266 (2019).
42. Krödel, M. et al. Rational design of ion exchange membrane material properties limits the crossover of $CO_2$ reduction products in artificial photosynthesis devices. *ACS Appl. Mater. Interfaces* **12**, 12030–12042 (2020).
43. Nishimura, Y. et al. Solid polymer electrolyte $CO_2$ reduction. *Energy Convers. Manag.* **36**, 629–632 (1995).
44. Narayanan, S. R., Haines, B., Soler, J. & Valdez, T. I. Electrochemical conversion of carbon dioxide to formate in alkaline polymer electrolyte membrane cells. *J. Electrochem. Soc.* **158**, A167–A173 (2011).
45. Aeshala, L. M., Rahman, S. U. & Verma, A. Effect of solid polymer electrolyte on electrochemical reduction of $CO_2$. *Sep. Purif. Technol.* **94**, 131–137 (2012).
46. Li, Y. C. et al. Bipolar membranes inhibit product crossover in $CO_2$ electrolysis cells. *Adv. Sustain. Syst.* **2**, 1700187 (2018).
47. Reyes, A. et al. Managing hydration at the cathode enables efficient $CO_2$ electrolysis at commercially relevant current densities. *ACS Energy Lett.* **5**, 1612–1618 (2020).
48. Weng, L.-C., Bell, A. T. & Weber, A. Z. Towards membrane-electrode assembly systems for $CO_2$ reduction: a modeling study. *Energy Environ. Sci.* **12**, 1950–1968 (2019).
49. Leonard, M. E., Clarke, L. E., Forner-Cuenca, A., Brown, S. M. & Brushett, F. R. Investigating electrode flooding in a flowing electrolyte, gas-fed carbon dioxide electrolyzer. *ChemSusChem* **89**, 400–411 (2019).
50. Dinh, C.-T. et al. $CO_2$ electroreduction to ethylene via hydroxide-mediated copper catalysis at an abrupt interface. *Science* **360**, 783–787 (2018).
51. Salvatore, D. & Berlinguette, C. P. Voltage matters when reducing $CO_2$ in an electrochemical flow cell. *ACS Energy Lett.* **5**, 215–220 (2020).
**Perspective paper that employs a reference electrode in situ of zero-gap $CO_2$ electrolysers to measure voltage drops across membrane electrode assembly components.**
52. Liu, Z. et al. Electrochemical generation of syngas from water and carbon dioxide at industrially important rates. *J. CO2 Util.* **15**, 50–56 (2016).
53. Liu, Z., Yang, H., Kutz, R. & Masel, R. I. $CO_2$ electrolysis to CO and $O_2$ at high selectivity, stability and efficiency using sustainion membranes. *J. Electrochem. Soc.* **165**, J3371 (2018).
54. Jiang, K. et al. Isolated Ni single atoms in graphene nanosheets for high-performance $CO_2$ reduction. *Energy Environ. Sci.* https://doi.org/10.1039/C7EE03245E (2018).
55. Zheng, T. et al. Large-scale and highly selective $CO_2$ electrocatalytic reduction on nickel single-atom catalyst. *Joule* **3**, 265–278 (2019).
56. Peng, H. et al. Alkaline polymer electrolyte fuel cells stably working at 80 °C. *J. Power Sources* **390**, 165–167 (2018).
57. Park, E. J. & Kim, Y. S. Quaternized aryl ether-free polyaromatics for alkaline membrane fuel cells: synthesis, properties, and performance — a topical review. *J. Mater. Chem. A* **6**, 15456–15477 (2018).
58. Luo, X., Rojas-Carbonell, S., Yan, Y. & Kusoglu, A. Structure–transport relationships of poly(aryl piperidinium) anion-exchange membranes: effect of anions and hydration. *J. Membr. Sci.* **598**, 117680 (2019).
59. Lee, J., Lim, J., Roh, C.-W., Whang, H. S. & Lee, H. Electrochemical $CO_2$ reduction using alkaline membrane electrode assembly on various metal electrodes. *J. CO2 Util.* **31**, 244–250 (2019).
60. Arquer, F. P. G. et al. $CO_2$ electrolysis to multicarbon products at activities greater than 1 A $cm^{-2}$. *Science* **367**, 661–666 (2020).
61. Xu, Y. et al. Oxygen-tolerant electroproduction of $C_2$ products from simulated flue gas. *Energy Environ. Sci.* **13**, 554–561 (2020).
62. Khadke, P. S. & Krewer, U. Mass-transport characteristics of oxygen at Pt/anion exchange ionomer interface. *J. Phys. Chem. C.* **118**, 11215–11223 (2014).
63. Zhang, T. et al. Nickel–nitrogen–carbon molecular catalysts for high rate $CO_2$ electro-reduction to CO: on the role of carbon substrate and reaction chemistry. *ACS Appl. Energy Mater.* **3**, 1617–1626 (2020).
64. Carter, B. M., Keller, L., Wessling, M. & Miller, D. J. Preparation and characterization of crosslinked poly(vinylimidazolium) anion exchange membranes for artificial photosynthesis. *J. Mater. Chem. A* https://doi.org/10.1039/C9TA00498J (2019).
65. Cui, L. et al. Novel sulfonated poly(ether ether ketone)/silica coated carbon nanotubes high-performance composite membranes for direct methanol fuel cell. *Polym. Adv. Technol.* **26**, 457–464 (2015).
66. Su, Y.-H. et al. Proton exchange membranes modified with sulfonated silica nanoparticles for direct methanol fuel cells. *J. Membr. Sci.* **296**, 21–28 (2007).
67. Si, K. et al. Rigid-rod poly(phenylenesulfonic acid) proton exchange membranes with cross-linkable biphenyl groups for fuel cell applications. *Macromolecules* **46**, 422–433 (2013).
68. Weissbach, T. et al. Simultaneous, synergistic control of ion exchange capacity and cross-linking of sterically-protected poly(benzimidazolium) s. *Chem. Mater.* **28**, 8060–8070 (2016).
69. Zhao, Y. et al. High-performance alkaline fuel cells using crosslinked composite anion exchange membrane. *J. Power Sources* **221**, 247–251 (2013).
70. Katzfuß, A. et al. Methylated polybenzimidazole and its application as a blend component in covalently cross-linked anion-exchange membranes for DMFC. *J. Membr. Sci.* **465**, 129–137 (2014).
71. Park, A. M., Turley, F. E., Wycisk, R. J. & Pintauro, P. N. Electrospun and cross-linked nanofiber composite anion exchange membranes. *Macromolecules* **47**, 227–235 (2014).
72. Weng, L.-C., Bell, A. T. & Weber, A. Z. Modeling gas-diffusion electrodes for $CO_2$ reduction. *Phys. Chem. Chem. Phys.* **20**, 16973–16984 (2018).
73. Mohanty, A. D., Tignor, S. E., Krause, J. A., Choe, Y.-K. & Bae, C. Systematic alkaline stability study of polymer backbones for anion exchange membrane applications. *Macromolecules* **49**, 3361–3372 (2016).
74. Arges, C. G. & Ramani, V. Investigation of cation degradation in anion exchange membranes using multi-dimensional NMR spectroscopy. *J. Electrochem. Soc.* **160**, F1006–F1021 (2013).
75. Parrondo, J., Wang, Z., Jung, M.-S. J. & Ramani, V. Reactive oxygen species accelerate degradation of anion exchange membranes based on polyphenylene oxide in alkaline environments. *Phys. Chem. Chem. Phys.* **18**, 19705–19712 (2016).
76. Klingele, M. et al. A completely spray-coated membrane electrode assembly. *Electrochem. Commun.* **70**, 65–68 (2016).
77. Breitwieser, M., Klingele, M., Vierrath, S., Zengerle, R. & Thiele, S. Tailoring the membrane–electrode interface in PEM fuel cells: a review and perspective on novel engineering approaches. *Adv. Energy Mater.* **8**, 1701257 (2018).
**Review and perspective paper on engineering the membrane–electrode interface to increase efficiency for PEM fuel cells; many of the same principles can be carried over to $CO_2$ electrolysers.**
78. Ito, H. et al. Experimental investigation of electrolytic solution for anion exchange membrane water electrolysis. *Int. J. Hydrogen Energy* **43**, 17030–17039 (2018).
79. Li, J., Li, X., Gunathunge, C. M. & Waegele, M. M. Hydrogen bonding steers the product selectivity of electrocatalytic CO reduction. *Proc. Natl Acad. Sci. USA* **116**, 9220–9229 (2019).
80. Ovalle, V. J. & Waegele, M. M. Understanding the impact of *N*-arylpyridinium ions on the selectivity of $CO_2$ reduction at the Cu/electrolyte interface. *J. Phys. Chem. C* **123**, 24453–24460 (2019).
81. Aeshala, L. M., Uppaluri, R. G. & Verma, A. Effect of cationic and anionic solid polymer electrolyte on direct electrochemical reduction of gaseous $CO_2$ to fuel. *J. CO2 Util.* **3-4**, 49–55 (2013).
82. Hou, P., Wang, X., Wang, Z. & Kang, P. Gas phase electrolysis of carbon dioxide to carbon monoxide using nickel nitride as the carbon enrichment catalyst. *ACS Appl. Mater. Interfaces* **10**, 38024–38031 (2018).
83. Ma, C. et al. Carbon nanotubes with rich pyridinic nitrogen for gas phase $CO_2$ electroreduction. *Appl. Catal. B* **250**, 347–354 (2019).
84. Ju, W. et al. Electrocatalytic reduction of gaseous $CO_2$ to CO on Sn/Cu-nanofiber-based gas diffusion electrodes. *Adv. Energy Mater.* **9**, 1901514 (2019).
85. Endrődi, B. et al. Multilayer electrolyzer stack converts carbon dioxide to gas products at high pressure with high efficiency. *ACS Energy Lett.* **4**, 1770–1777 (2019).
86. Jeong, H.-Y. et al. Achieving highly efficient $CO_2$ to CO electroreduction exceeding 300 mA $cm^{-2}$ with single-atom nickel electrocatalysts. *J. Mater. Chem. A* **7**, 10651–10661 (2019).
87. Zhu, W., Kattel, S., Jiao, F. & Chen, J. G. Shape-controlled $CO_2$ electrochemical reduction on nanosized Pd hydride cubes and octahedra. *Adv. Energy Mater.* **9**, 1802840 (2019).

88. Wang, Y. et al. Catalyst synthesis under $CO_2$ electroreduction favours faceting and promotes renewable fuels electrosynthesis. *Nat. Catal.* **3**, 98–106 (2020).
89. Li, F. et al. Molecular tuning of $CO_2$-to-ethylene conversion. *Nature* **577**, 509–513 (2020).
90. Kaczur, J. J., Yang, H., Liu, Z., Sajjad, S. D. & Masel, R. I. Carbon dioxide and water electrolysis using new alkaline stable anion membranes. *Front. Chem.* **6**, 263 (2018).

## Competing interests
The authors declare no competing interests.

## Additional information
**Supplementary Information** The online version contains supplementary material available at https://doi.org/10.1038/s41560-020-00761-x.

**Correspondence** should be addressed to C.P.B.

**Peer review information** *Nature Energy* thanks Zengcai Liu, Guenter Schmid and the other, anonymous, reviewer(s) for their contribution to the peer review of this work.

**Reprints and permissions information** is available at www.nature.com/reprints.

**Publisher's note** Springer Nature remains neutral with regard to jurisdictional claims in published maps and institutional affiliations.